Exact time-dependent analytical solutions for entropy production rate in a system operating in a heat bath in which temperature varies linearly in space

Mesfin Asfaw Taye[*]

West Los Angeles College, Science Division 9000 Overland Ave, Culver City, California 90230, USA

The nonequilibrium thermodynamics feature of a Brownian motor is investigated by obtaining exact time-dependent solutions. This in turn enables us to investigate not only the long time property (steady state) but also the short time the behavior of the system. The general expressions for the free energy, entropy production $\dot{e}_p(t)$ as well as entropy extraction $\dot{h}_d(t)$ rates are derived for a system that is genuinely driven out of equilibrium by time-independent force as well as by spatially varying thermal background. We show that for a system that operates between hot and cold reservoirs, most of the thermodynamics quantities approach a nonequilibrium steady state in the long time limit. The change in free energy becomes minimal at a steady state. However, for a system that operates in a heat bath where its temperature varies linearly in space, the entropy production and extraction rates approach a nonequilibrium steady state while the change in free energy varies linearly in space. This reveals that unlike systems at equilibrium, when systems are driven out of equilibrium, their free energy may not be minimized. The thermodynamic properties of a system that operates between the hot and cold baths are further compared and contrasted with a system that operates in a heat bath where its temperature varies linearly in space along with the reaction coordinate. We show that the entropy, entropy production, and extraction rates are considerably larger for the linearly varying temperature case than a system that operates between the hot and cold baths revealing such systems are inherently irreversible. For both cases, in the presence of load or when a distinct temperature difference is retained, the entropy $S(t)$ monotonously increases with time and saturates to a constant value as t further steps up. The entropy production rate $\dot{e}_p$ decreases in time and at steady state, $\dot{e}_p = \dot{h}_d > 0$, which agrees with the results shown in M. Asfaw's [Phys. Rev. E **89**, 012143 (2014); **92**, 032126 (2015)]. Moreover, the velocity, as well as the efficiency of the system that operates between the hot and cold baths, are also collated and contrasted with a system that operates in a heat bath where its temperature varies linearly in space along with the reaction coordinate. A system that operates between the hot and cold baths has significantly lower velocity but a higher efficiency in comparison with a linearly varying temperature case.

I. INTRODUCTION

Thermodynamics is one of the most studied disciplines since its applications encompass a variety of topics in science and engineering. It can be further subdivided into equilibrium and nonequilibrium disciplines. Equilibrium thermodynamics is well studied but has limited applications since most systems in nature are far from equilibrium. In this case, its macroscopic properties can be further verified from a microscopic point of view via equilibrium statistical mechanics. In contrast, nonequilibrium thermodynamics deals with inhomogeneous systems where the system thermodynamic quantities rely on the reaction rates in a complicated manner. As a result, getting a universal exact result was unattainable. However, in the last few decades, several studies have been conducted to explore the nonequilibrium thermodynamic feature of systems that are out of equilibrium [1–17]. Some notable works in this regard include the analytically solvable models depicted in Refs. [18,19] and the study of thermodynamic features for systems that operate in the quantum realm [20–22]. Furthermore, for systems that are genuinely driven out of equilibrium, the

thermodynamic relations were derived for a Brownian particle that walks in an overdamped medium [23] and underdamped medium [24]. The method of calculating entropy production and extraction rates at the ensemble level by first analyzing the thermodynamic relation at trajectory level was introduced in Ref. [6]. Alternatively, many thermodynamic relations were reconfirmed under time reversal operation [25,26]. Such studies help to comprehend the thermodynamic properties of biological systems such as intracellular transport of kinesin or dynein inside the cell [27–29].

Since real systems operate in a finite time, solving the model system exactly as a function of time is fundamental to grasp the thermodynamic features of the systems beyond a linear response and steady-state regimes. In this work by obtaining exact time-dependent solutions, we investigate not only the long time property (steady state) but also the short time behavior of the system. The general expressions for free energy, entropy production, as well as entropy production rates are derived for a system that is genuinely driven out of equilibrium by time-independent force as well as by spatially varying thermal background. By solving the model as a function of time, the dependence of these thermodynamic quantities as a function of time is explored. For a system that operates between hot and cold reservoirs, most of these

_____

[*]tayem@wlac.edu

thermodynamics quantities approach a nonequilibrium steady state in the long time limit. The change in free energy becomes minimal at a steady state. However for a system that operates in a heat bath where its temperature decreases linearly, the entropy production and extraction rates approach a nonequilibrium steady state while the change in the free energy decreases linearly. This reveals that unlike systems at equilibrium, when systems are driven out of equilibrium, their free energy may keep decreasing as time evolves. In the absence of load and isothermal cases, we show that the nonequilibrium state relaxes to equilibrium.

In this work, we also consider a simple model where the single-particle walks in one-dimensional discrete ratchet potential with a load. The ratchet potential is also coupled with a heat bath. The thermodynamic properties of a system that operates between the hot and cold baths are compared and contrasted with a system that operates in a heat bath where its temperature linearly decreases along with the reaction coordinate. We show that the entropy $S(t)$, the entropy production $\dot{e}_p(t)$, and extraction rates $\dot{h}_d(t)$ are considerably larger for a linearly decreasing temperature case than a Brownian particle that operates between the hot and cold baths revealing such systems are inherently irreversible. For both cases, in the presence of load or when a distinct temperature difference is retained, the entropy $S(t)$ monotonously increases with time and saturates to a constant value as t further steps up. The entropy production rate $\dot{e}_p$ decreases in time and at steady state, $\dot{e}_p = \dot{h}_d > 0$ which agrees with the results shown in Refs. [18,19]. On the contrary, for an isothermal case and in the absence of load, $\dot{e}_p = \dot{h}_d = 0$ in a long time limit, which is a reasonable argument as any system that is in contact with a uniform temperature should obey the detail balance condition.

Because closed-form expressions for $\dot{S}(t)$, $\dot{e}_p(t)$, and $\dot{h}_d(t)$ as a function of t are obtained, the analytic expressions for the change in entropy production $\Delta e_p(t)$, heat dissipation $\Delta h_d(t)$, and total entropy $\Delta S(t)$ can be found. We show that for a system that operates between hot and cold reservoirs, $\Delta h_d(t)$ and $\Delta e_p(t)$ approach a nonequilibrium steady state in the long time limit. However, for a system that operates in heat baths where its temperature decreases linearly, $\Delta h_d(t)$ and $\Delta e_p(t)$ increase linearly as time progresses. In the absence of a load, potential barrier, and for the isothermal case, for both cases, $\Delta S = \ln[3]$, which reconfirms the well-known relation for a system under infinitesimal process. In other words, since the system has three accessible states (three lattices) $\Omega = 3$, at equilibrium $S = \ln(\Omega)$. At equilibrium one also finds, $\dot{e}_p(t) = \ln[3]$ and $\dot{h}_d(t) = 0$. Moreover, the change in free energy ΔF decreases in time and saturates to a constant but minimal value for the system that operates between the hot and cold baths. On the contrary, for the system that operates in a linearly decreasing temperature case, the free energy decreases linearly.

The velocity, as well as the efficiency of the system that operates between the hot and cold baths, are also compared and contrasted with a system that operates in a heat bath where its temperature linearly decreases along with the reaction coordinate. A system that operates between the hot and cold baths has significantly lower velocity but a higher efficiency in comparison with a linearly decreasing temperature case. For a linearly decreasing temperature case, we show that the effi-

ciency of such a Brownian heat engine is far less than Carnot's efficiency even at the quasistatic limit. At quasistatic limit, the efficiency of the heat engine approaches the efficiency of an endoreversible engine $\eta = 1 - \sqrt{T_c/T_h}$ [30]. Moreover, the dependence of the current, as well as the efficiency on the model parameters, is explored analytically.

The rest of the paper is organized as follows: in Sec. II, we present the model and derive the expression for various thermodynamic relations for a Brownian particle walks in one-dimensional discrete ratchet potential with a load. In Sec. III, the role of time on entropy and free energy is explored. In Sec. IV, the dependence of efficiency and velocity on model parameters is explored. Section V deals with the summary and conclusion.

II. THE MODEL AND DERIVATION OF FREE ENERGY

In this section, we derive the general expression for free energy, entropy production, as well as entropy production rates for a system that is driven out of equilibrium by time-independent force as well as a spatially varying thermal background. By solving the model as a function of time, we explore the dependence of these thermodynamic quantities as a function of time. Let us now consider a Brownian particle that moves in a discrete lattice where its dynamics is governed by the master equation [18]

$$\frac{dP_n}{dt} = \sum_{n \neq n'} (P_{nn'} p_{n'} - P_{n'n} p_n), \quad n, n' = 1, 2, 3. \quad (1)$$

Here $P_{n'n}$ is the transition probability rate at which the system, originally in state n, makes a transition to state n'. $P_{n'n}$ is given by the Metropolis rule [18]. Next, the relation for the entropy production rate as well as the free energy will be explored as a function of time by considering a Brownian particle that moves along the one-dimensional discrete ratchet potential.

Case 1: Brownian particle operating between hot and cold reservoirs. Before considering a linearly decreasing temperature profile, for clarity let us first rederive the entropy production rate for a Brownian particle that moves in the one-dimensional discrete ratchet potential U_i [18]

$$U_i = E[i(\text{mod}3 - 1] + ifd. \quad (2)$$

The ratchet potential is coupled with the temperature

$$T_i = \begin{cases} T_h, & \text{if } E[i(\text{mod}3 - 1] = 0; \\ T_c, & \text{otherwise}; \end{cases} \quad (3)$$

as shown in Fig. 1. The potential $E > 0$, f denotes the load and i is an integer that runs from $-\infty$ to ∞. T_h and T_c designate the temperature for the hot and cold reservoirs, respectively. Moreover, d denotes the lattice spacing d and in one cycle, the particle walks a net displacement of three lattice sites as shown in Fig. 1. The jump probability from site i to $i + 1$ is given by $\Gamma e^{-\Delta E/k_B T_i}$ where $\Delta E = U_{i+1} - U_i$ and Γ is the probability attempting a jump per unit time. k_B designates the Boltzmann constant and hereafter k_B, Γ and d are considered to be a unity. Obeying the metropolis algorithm when $\Delta E \leqslant 0$, the jump definitely takes place while $\Delta E > 0$ the jump takes place with probability $\exp(-\Delta E/T_i)$ [14]. Substituting the probability rates [see Eq. (6)] into Eq. (1)
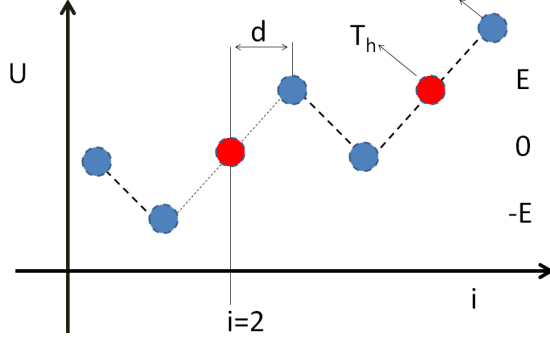
FIG. 1. Schematic diagram for a Brownian particle walking in a discrete ratchet potential with load. Sites with red circles are coupled to the hot reservoir (T_h) while sites with blue circles are coupled to the cold reservoir (T_c). Site 1 is labeled explicitly and d is the lattice spacing.

yields

$$\frac{d\vec{p}}{dt} = \mathbf{P}\vec{p}, \tag{4}$$

where $\vec{p} = (p_1, p_2, p_3)^T$. $\mathbf{P}$ is a 3 by 3 matrix which is given by

$$\mathbf{P} = \begin{pmatrix} \frac{-\mu a^2 - \mu^2}{2a} & \frac{1}{2} & \frac{1}{2} \\ \frac{\mu a}{2} & \frac{-1 - vb}{2} & \frac{1}{2} \\ \frac{\mu^2}{2a} & \frac{vb}{2} & -1 \end{pmatrix}, \tag{5}$$

as long as $0 < f < 2E$. Here $\mu = e^{-E/T_c}$, $v = e^{-E/T_h}$, $a = e^{-f/T_c}$ and $b = e^{-f/T_h}$. It is important to note that via the expressions $p_1(t)$, $p_2(t)$ and $p_3(t)$ that are shown in Appendix A and using the rates

$$P_{21} = \tfrac{1}{2}e^{-(E+f)/T_c}, \; P_{12} = \tfrac{1}{2}, \; P_{32} = \tfrac{1}{2}e^{-(E+f)/T_h}$$
$$P_{23} = \tfrac{1}{2}, P_{13} = \tfrac{1}{2}, P_{31} = \tfrac{1}{2}e^{-(2E-f)/T_c}, \tag{6}$$

the thermodynamic quantities that are under investigation can be evaluated.

The net velocity $V(t)$ at any time t is the difference between the forward $V_i^+(t)$ and backward $V_i^-(t)$ velocities at each site i

$$V(t) = \sum_{i=1}^{3}(V_i^+(t) - V_i^-(t))$$
$$= (p_1 P_{21} - p_2 P_{12}) + (p_2 P_{32} - p_3 P_{23})$$
$$+ (p_3 P_{13} - p_1 P_{31}). \tag{7}$$

At stall force

$$f = \frac{E\left(\frac{T_h}{T_c} - 1\right)}{\left(\frac{2T_h}{T_c} + 1\right)}, \tag{8}$$

the velocity approaches zero.

Let us next derive the fundamental entropy relation

$$S[p_i(t)] = -\sum_{i=1}^{3} p_i \ln p_i, \tag{9}$$

for the system that is far from equilibrium. Since the hot heat bath located at $i = 2$ loses $(E + f)$ amount of heat to the lattice $i = 3$ and at the same time gains $(E + f)$ amount of heat from the lattice $i = 3$, one can write the heat per unit time taken from the hot reservoir is given as

$$\dot{Q}_h(t) = (E + f)(p_2 P_{32} - p_3 P_{23})$$
$$= T_h(p_2 P_{32} - p_3 P_{23}) \ln\left(\frac{P_{32}}{P_{23}}\right), \tag{10}$$

as shown in Ref. [19]. Note that $\ln(\frac{P_{32}}{P_{23}}) = (E + f)/T_h$. On the other hand, the heat per unit time given to cold reservoir is given by

$$\dot{Q}_c(t) = (E + f)(p_2 P_{12} - p_1 P_{21})$$
$$+ (2E - f)(p_3 P_{13} - p_1 P_{31})$$
$$= T_c(p_2 P_{12} - p_1 P_{21}) \ln\left(\frac{P_{12}}{P_{21}}\right)$$
$$+ T_c(p_3 P_{13} - p_1 P_{31}) \ln\left(\frac{P_{13}}{P_{31}}\right). \tag{11}$$

Let us write the entropy extraction (heat dissipation) rate

$$\dot{h}_d(t) = \frac{-\dot{Q}_h(t)}{T_h} + \frac{\dot{Q}_c(t)}{T_c}. \tag{12}$$

Substituting Eqs. (10) and (11) into Eq. (12) leads to

$$\dot{h}_d(t) = \frac{-\dot{Q}_h(t)}{T_h} + \frac{\dot{Q}_c(t)}{T_c}$$
$$= \sum_{i>j}(p_i P_{ji} - p_j P_{ij}) \ln\left(\frac{P_{ji}}{P_{ij}}\right)$$
$$= \sum_{i>j}(p_i P_{ji} - p_j P_{ij}) \ln\left(\frac{p_i P_{ji}}{p_j P_{ij}}\right)$$
$$- \sum_{i>j}(p_i P_{ji} - p_j P_{ij}) \ln\left(\frac{p_i}{p_j}\right)$$
$$= \dot{e}_p(t) - \dot{S}(t), \tag{13}$$

where

$$\dot{e}_p(t) = \sum_{i>j}(p_i P_{ji} - p_j P_{ij}) \ln\left(\frac{p_i P_{ji}}{p_j P_{ij}}\right) \tag{14}$$

and

$$\dot{S}(t) = \sum_{i>j}(p_i P_{ji} - p_j P_{ij}) \ln\left(\frac{p_i}{p_j}\right). \tag{15}$$

Here $\dot{e}_p(t)$ and $\dot{S}(t)$ denote the internal entropy production rate and the change in the entropy. From Eq. (15), one derives $S[p_i(t)] = -\sum_{i=1}^{3} p_i \ln p_i$ which implies the fundamental entropy equation is still valid for the systems that are driven out of equilibrium.

Case 2: Linearly decreasing temperature. Let us now consider a single Brownian particle that hops along the one-dimensional discrete ratchet potential [see Eq. (2)] with a load
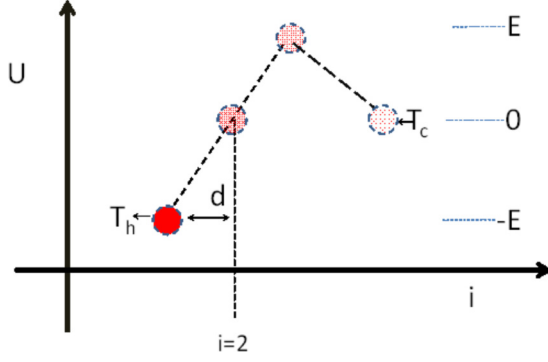
FIG. 2. The schematic diagram for a Brownian particle that walks in a discrete ratchet potential coupled with a linearly decreasing temperature profile. The temperature for the heat baths decreases from T_h to T_c according to Eq. (16).

that coupled with a linearly decreasing temperature [14]

$$T_i = T_h + \frac{(i-1)(T_c - T_h)}{3}, \tag{16}$$

as shown in Fig. 2. The indexes $i = 1 \cdots 3$. Once again, the rate equation for the model is given by $\frac{d\vec{p}}{dt} = \mathbf{P}\vec{p}$ where $\vec{p} = (p_1, p_2, p_3)^T$. $\mathbf{P}$ is a 3 by 3 matrix which is given by

$$\mathbf{P} = \begin{pmatrix} -\frac{a\mu_1}{2} - \frac{\mu_2^2}{2a_2} & \frac{1}{2} & \frac{1}{2} \\ \frac{a\mu_1}{2} & \frac{1}{2}(-1-\nu) & \frac{1}{2} \\ \frac{\mu_2^2}{2a_2} & \frac{\nu}{2} & -1 \end{pmatrix}, \tag{17}$$

as long as $0 < f < 2E$. Here $\mu_1 = e^{-E/T_1}$, $\nu = e^{-(E+f)/T_2}$, $a_1 = e^{-f/T_1}$, $\mu_2 = e^{-E/T_4}$ and $a_2 = e^{-f/T_4}$. Since the temperature linearly decreases, the parameter $T_1 = T_h$, $T_2 = T_h + (T_c - T_h)/3$, $T_3 = T_h + 2(T_c - T_h)/3$ and $T_4 = T_c$. The sum of each column of the matrix $\mathbf{P}$ is zero, $\sum_m \mathbf{P}_{mn} = 0$ which reveals that the total probability is conserved: $(d/dt)\sum_n p_n = d/dt(\mathbf{1}^T \cdot p) = \mathbf{1}^T \cdot (\mathbf{P}\vec{p}) = 0$. It is important to note that via the expressions $p_1(t)$, $p_2(t)$, and $p_3(t)$ that are shown in Appendix B and using the rates

$$P_{21} = \frac{1}{2}e^{-(E+f)/T_1} \quad P_{12} = \frac{1}{2}, \quad P_{32} = \frac{1}{2}e^{-(E+f)/T_2}$$
$$P_{23} = \frac{1}{2}, P_{13} = \frac{1}{2}, P_{31} = \frac{1}{2}e^{-(2E-f)/T_4}, \tag{18}$$

the thermodynamic quantities which are under investigation can be evaluated.

Once again, the velocity $V(t)$ at any time t is the difference between the forward $V_i^+(t)$ and backward $V_i^-(t)$ velocities at each site i

$$V(t) = \sum_{i=1}^{3}(V_i^+(t) - V_i^-(t))$$
$$= (p_1 P_{21} - p_2 P_{12}) + (p_2 P_{32} - p_3 P_{23})$$
$$+ (p_3 P_{13} - p_1 P_{31}). \tag{19}$$

At stall force

$$f = \frac{E(T_h - T_c)(4T_h + T_c)}{(2T_h^2 + T_c^2 + 6T_c T_h)}, \tag{20}$$

the velocity approaches zero.

The previously derived relation for the entropy production rate

$$\dot{e}_p(t) = \sum_{i>j}(p_i P_{ji} - p_j P_{ij}) \ln\left(\frac{p_i P_{ji}}{p_j P_{ij}}\right), \tag{21}$$

the entropy extraction rate

$$\dot{h}_d(t) = \sum_{i>j}(p_i P_{ji} - p_j P_{ij}) \ln\left(\frac{P_{ji}}{P_{ij}}\right), \tag{22}$$

and the rate of total entropy

$$\dot{S}(t) = \sum_{i>j}(p_i P_{ji} - p_j P_{ij}) \ln\left(\frac{p_i}{p_j}\right) \tag{23}$$

are still valid regardless of any parameter choice. For both cases, as steady state $\dot{e}_p(t) = \dot{h}_d(t)$. In the absence of load f and in the limit $T_h \to T_c$ (when the system relaxes to its equilibrium state), for both cases, one finds

$$\dot{h}_d(t) = 0 \tag{24}$$

and

$$\dot{e}_p(t) = \dot{S}(t) = -e^{\frac{-3t}{2}} \ln\left[\frac{-1 + e^{\frac{3t}{2}}}{2 + e^{\frac{3t}{2}}}\right] \tag{25}$$

as long as $E = 0$. At stationary state (at equilibrium) $t \to \infty$, $\dot{e}_p(t) = \dot{h}_d(t) = \dot{S}(t) = 0$.

Because closed-form expressions for $\dot{S}(t)$, $\dot{e}_p(t)$, and $\dot{h}_d(t)$ as a function of t are obtained, the analytic expressions for the change in entropy production, heat dissipation, and total entropy can be found analytically via

$$\Delta h_d(t) = \int_{t_0}^{t}(\dot{h}_d(t))dt, \tag{26}$$

$$\Delta e_p(t) = \int_{t_0}^{t}(\dot{e}_p(t))dt, \tag{27}$$

and

$$\Delta S(t) = \int_{t_0}^{t}(\dot{S}(t))dt, \tag{28}$$

where $\Delta S(t) = \Delta e_p(t) - \Delta h_d(t)$ and the indexes $i = 1 \cdots 3$ and $j = 1 \cdots 3$. Once again, in the absence of load f, in the limit $T_h \to T_c$ and when $E = 0$, for both cases, one finds

$$\Delta h_d(t) = 0, \tag{29}$$

$$\Delta S(t) = \Delta e_p(t) = -\frac{1}{6}(-9t - 6\ln[3] + 4\ln[-1 + e^{3t/2}])$$
$$-\frac{1}{6}\left(+2\ln[2 + e^{3t/2}] - 4e^{-3t/2}\ln\left[1 - \frac{3}{2 + e^{3t/2}}\right]\right). \tag{30}$$

As expected, in the limit $t \to \infty$, the system approaches equilibrium state and Eq. (30) converges to

$$\Delta S = \Delta e_p(t) = \ln[3], \tag{31}$$

which reconfirm the the well-known relation for system under infinitesimal process. In other words, the system has three

accessible states (three lattices) $\Omega = 3$ and at equilibirium $S = \ln(\Omega)$.

Furthermore, for linearly decreasing temperature case, the heat dissipation rate is rewritten as

$$
\begin{aligned}
\dot{H}_d(t) &= \sum_{i>j} T_j(p_i P_{ji} - p_j P_{ij}) \ln\left(\frac{P_{ji}}{P_{ij}}\right) \\
&= \sum_{i>j} T_j(p_i P_{ji} - p_j P_{ij}) \ln\left(\frac{p_i P_{ji}}{p_j P_{ij}}\right) \\
&\quad - \sum_{i>j} T_j(p_i P_{ji} - p_j P_{ij}) \ln\left(\frac{p_i}{p_j}\right) \\
&= \dot{E}_p(t) - \dot{S}^T(t),
\end{aligned}
\tag{32}
$$

where

$$
\dot{E}_p(t) = \sum_{i>j} T_j(p_i P_{ji} - p_j P_{ij}) \ln\left(\frac{p_i P_{ji}}{p_j P_{ij}}\right)
\tag{33}
$$

and

$$
\dot{S}^T(t) = \sum_{i>j} T_j(p_i P_{ji} - p_j P_{ij}) \ln\left(\frac{p_i}{p_j}\right).
\tag{34}
$$

Here the indexes $i = 1 \cdots 3$ and $j = 1 \cdots 3$. Our next objective is to write the expression for the free energy in terms of $\dot{E}_p(t)$ and $\dot{H}_d(t)$ where $\dot{E}_p(t)$ and $\dot{H}_d(t)$ are the terms that are associated with $\dot{e}_p(t)$ and $\dot{h}_d(t)$ except the temperature T_j. Now we have entropy balance equation $\dot{S}^T(t) = \dot{E}_p(t) - \dot{H}_d(t)$ for our model system. For isothermal case and in the absence of load, the system relaxes to its equilibrium. For the case $E = 0$, one finds $\dot{H}_p(t) = 0$ and

$$
\dot{E}_p(t) = \dot{S}^T(t) = T_c e^{\frac{-3t}{2}} \ln\left[\frac{-1 + e^{\frac{3t}{2}}}{2 + e^{\frac{3t}{2}}}\right].
\tag{35}
$$

In the limit $t \to 0$, $\dot{E}_p(t) = \dot{S}^T(t) = 0$.

The second law of thermodynamics can be written as $\Delta S^T(t) = \Delta E_p(t) - \Delta H_d(t)$ where $\Delta S^T(t)$, $\Delta E_p(t)$ and $\Delta H_d(t)$ are very lengthy expressions that can be evaluated via

$$
\Delta H_d = \int_{t_0}^{t} (\dot{H}_d(t)) dt,
\tag{36}
$$

$$
\Delta E_p(t) = \int_{t_0}^{t} (\dot{E}_p(t)) dt,
\tag{37}
$$

and

$$
\Delta S^T(t) = \int_{t_0}^{t} (\dot{S}^T(t)) dt.
\tag{38}
$$

When $f = 0$, $T_h \to T_c$ and $E = 0$ (system approaching equilibirium), $\Delta H_d = 0$ for any time t while

$$
\begin{aligned}
\Delta S^T(t) &= \Delta E_p(t) \\
&= -T_c \frac{1}{6}(-9t - 6\ln[3] + 4\ln[-1 + e^{3t/2}]) \\
&\quad - T_c \frac{1}{6}\left(+2\ln[2 + e^{3t/2}] - 4e^{-3t/2}\ln\left[1 - \frac{3}{2 + e^{3t/2}}\right]\right).
\end{aligned}
\tag{39}
$$

In long time limit (at equilibirium), $\Delta S(t) = \Delta e_p(t) = T_c \ln[3]$.

On the other hand, the total internal energy $U(t)$ is the sum of the internal energies

$$
\begin{aligned}
U[p_i(t)] &= \sum_{i=1}^{3} p_i u_i \\
&= p_1(t)(-E) + p_3(t)(E),
\end{aligned}
\tag{40}
$$

while the change in the internal energy is given by

$$
\begin{aligned}
\Delta U(t) &= U[p_i(t)] - U[p_i(0)] \\
&= E(p_3(t) - p_3(0) + p_1(0) - p_1(t)).
\end{aligned}
\tag{41}
$$

We also verify the first law of thermodynamics

$$
\begin{aligned}
\dot{U}[P_i(t)] &= -\sum_{i>j}(p_i P_{ji} - p_j P_{ij})(u_i - u_j) \\
&= -(\dot{H}_d(t) + fV(t)).
\end{aligned}
\tag{42}
$$

Next let us find the expression for the free energy dissipation rate $\dot{F}$. For the isothermal case, the free energy is given by $F = U - TS$ and next we adapt this relationship to nonisothermal case to write

$$
\dot{F}(t) = \dot{U} - \dot{S}^T(t).
\tag{43}
$$

Substituting Eqs. (32) and (42) in Eq. (43) leads to

$$
\dot{F}(t) + \dot{E}_p(t) = \dot{U}(t) + \dot{H}_d(t) = -fV(t),
\tag{44}
$$

which is the second law of thermodynamics. Note that in the absence of load, $\dot{U}(t) = -\dot{H}_d(t)$ and consequently $\dot{E}_p(t) = -\dot{F}(t)$. The change in the free energy can be written as

$$
\begin{aligned}
\Delta F(t) &= -\int_{t_0}^{t}(fV(t) + \dot{E}_p(t)) dt \\
&= \int_{t_0}^{t}(\dot{U}(t) + \dot{H}_d(t) - \dot{E}_p(t)) dt \\
&= \Delta U + \Delta H_d - \Delta E_p.
\end{aligned}
\tag{45}
$$

As expected, at the quasistatic limit where the velocity approaches zero $V(t) = 0$, $\dot{E}_p(t) = 0$ and $\dot{H}_d(t) = 0$ and far from quasistatic limit $E_p > 0$, which is expected as the engine operates irreversibly. Far from stall force, $\dot{E}_p(t) \neq \dot{H}_d(t)$, as long as a distinct temperature difference between the hot reservoirs is retained.

For isothermal case, in the absence of potential barrier and load, $\Delta U = \Delta H_d = 0$ and $\Delta F(t) = -\Delta E_p$. At equilibrium ($t \to \infty$), we get $\Delta F = -T_c \ln(3)$. We can recheck this relation via the statistical mechanics approach. In the limit, $t \to \infty$, the probability distributions that are shown in Appendices A and B, converge

$$
P_1 = \frac{1}{1 + e^{-\frac{E}{T_c}} + e^{-\frac{2E}{T_c}}},
$$

$$
P_2 = \frac{e^{-\frac{E}{T_c}}}{1 + e^{-\frac{E}{T_c}} + e^{-\frac{2E}{T_c}}},
$$

$$
P_3 = \frac{e^{-\frac{2E}{T_c}}}{1 + e^{-\frac{E}{T_c}} + e^{-\frac{2E}{T_c}}}.
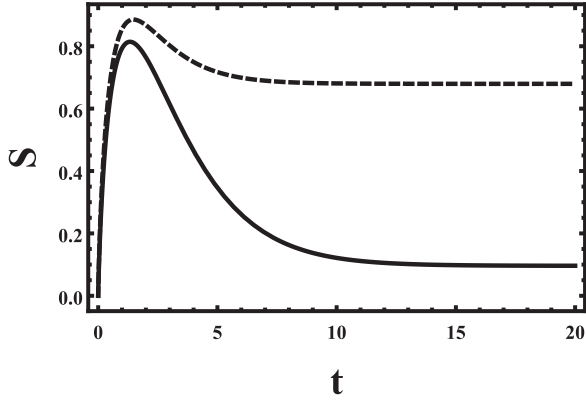\tag{46}
$$

FIG. 3. The entropy $S(t)$ as a function of t evaluated analytically via Eq. (9) for a given $\epsilon = 4.0$, $f = 0.0$ and $\tau = 2.0$. The dashed line indicates the plot for a heat bath where its temperature linearly decreases along with the reaction coordinate while the solid line is plotted by considering a Brownian particle that operates between the hot and cold baths.

Accordingly, the partition function is given by

$$Z = \sum_{i=1}^{3} e^{-\frac{E_i}{T_c}}$$

$$= 1 + e^{-\frac{E}{T_c}} + e^{-\frac{2E}{T_c}}. \tag{47}$$

The free energy as well the entropy can be calculated as $F = -T_c \ln(Z)$ and $S = \ln(z) + \bar{E}\beta$. When $E \to 0$, the free energy converges to $F = -T_c \ln(3)$ while the entropy approaches $S = \ln(3)$.

III. ENTROPY PRODUCTION RATE AND FREE ENERGY

Hereafter, whenever we plot the figures, we use dimensionless quantities $\epsilon = E/T_c$, $\lambda = f/T_c$ and $\tau = \frac{T_h}{T_c}$. We also introduce dimensionless time $\bar{t} = \Gamma t$ and after this the bar will be dropped.

Entropy. The dependence of entropy on the model parameters can be explored via Eq. (9). As shown in Fig. 3, the entropy of the system exhibits an intriguing parameter dependence.

As shown in the figure, for $t \neq 0$, $S > 0$ which indicates that in the presence of symmetry-breaking fields such as nonuniform temperature or external force, the system is driven out of equilibrium. $S(t)$ is also considerably larger for the linearly decreasing temperature case than the entropy for Brownian particle that operates between the hot and cold baths. This suggests that that the entropy production is higher for the system that operates in a heat bath where its temperature decreases linearly along with the reaction coordinate. For isothermal case $T_h = T_c$ as well as in the absence of both external load and bistable potential $U_0 = 0$, the particle undergoes a random walk on a lattice. For both cases, $S(t)$ converges to $S(t) \to \ln[3]$ in the limit $t \to \infty$.

Entropy production rate. Next let us explore the dependence for the rate of entropy production $\dot{e}_p(t)$, the rate of entropy $\dot{S}(t)$, and the rate of entropy flow from the system to the outside $\dot{h}_d(t)$ on the system parameters. The expression
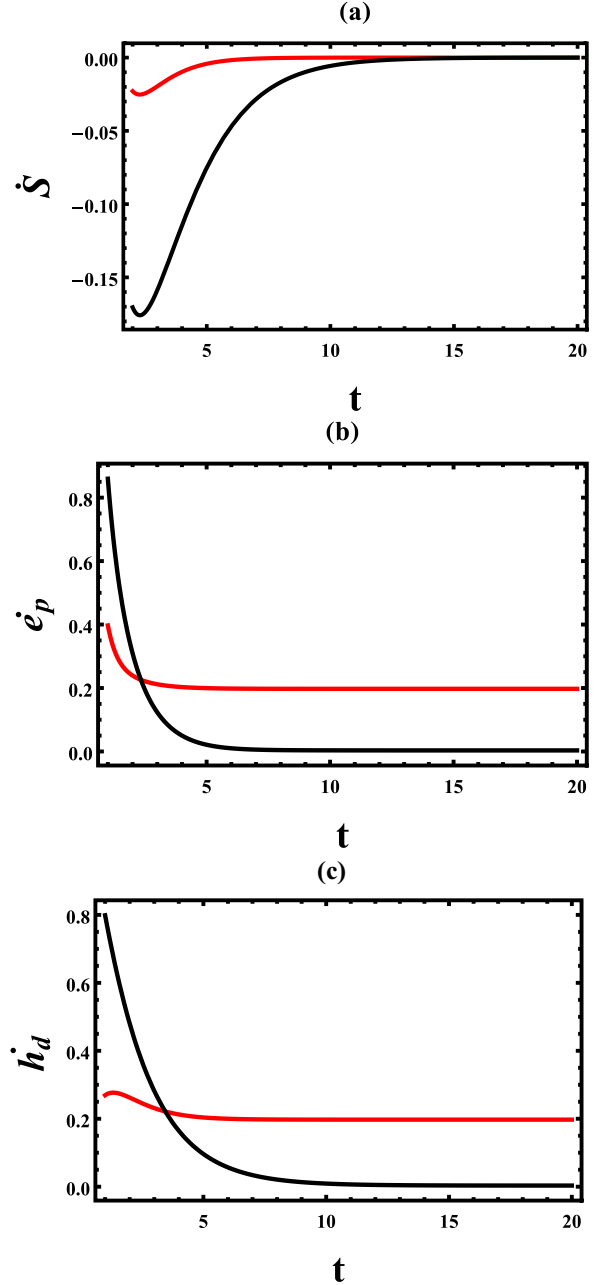

FIG. 4. (a) $\dot{S}(t)$ versus t is evaluated analytically via Eqs. (15) and (23). (b) The entropy production rate $\dot{e}_p(t)$ as a function of t. $\dot{e}_p(t)$ is analyzed analytically via Eqs. (14) and (21). (c) The entropy extraction rate $\dot{h}_d(t)$ as a function of t evaluated analytically using Eqs. (13) and (22). In the figures, the red line indicates the plot for a heat bath where its temperature linearly decreases while the black solid line is plotted by considering a Brownian particle that operates between the hot and cold baths. Clearly $\dot{h}_d(t)$ and $\dot{e}_p(t)$ are considerably large for linearly decreasing temperature case. In the figures, we fix $\epsilon = 2, 0$, $\tau = 20.0$, $\lambda = 0.6$.

for $\dot{S}(t)$, $\dot{h}_d(t)$, and $\dot{e}_p(t)$ can be evaluated via Eqs. (23), (22), and (21), respectively, as shown in Fig. 4. In the figure, we plot $\dot{S}(t)$, $\dot{h}_d(t)$, and $\dot{e}_p(t)$ as a function of t. In the figure, the red line indicates the plot for a heat bath where its temperature linearly decreases while the solid line is plotted by considering a Brownian particle that operates between the hot and cold
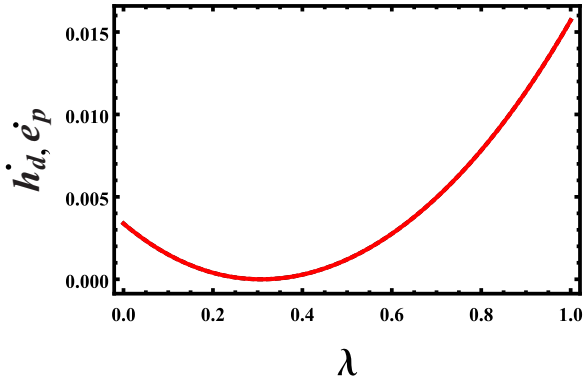
FIG. 5. The entropy production rate $\dot{e}_p(t)$ and the entropy extraction rate $\dot{h}_d(t)$ versus λ. The entropy production rate is analyzed via Eqs. (14) and (21) while the entropy extraction rate is evaluated analytically using Eqs. (13) and (22). In the figure, the parameters are fixed as $\epsilon = 2$, $\tau = 2.0$ and $t = 10^6$ (steady state). At steady state $\dot{e}_p(t) = \dot{h}_d(t)$.

baths. The fact that $\dot{e}_p(t) > 0$ and $\dot{h}_d(t) > 0$ exhibits that the system is exposed to symmetry-breaking fields such as external force or nonuniform temperature. As a result, the system is driven out of equilibrium. The entropy, entropy production, and extraction rates are also higher for linearly decreasing cases than the particle that operates between two heat baths indicating that a system that operates in a heat bath where its temperature decreases linearly with the reaction coordinate exhibits a higher level of irreversibility. As expected, $\dot{e}_p(t)$ and $\dot{h}_d(t)$ approach their steady-state values $\dot{e}_p = \dot{h}_d$ as time progresses. Even in the absence of symmetry-breaking fields, as long as the system is operating in a finite time, the system exhibits irreversible dynamics and as a result $\dot{e}_p > 0$ for small t and decreases (the system relaxes to equilibrium) as time increases. In the limit $t \to \infty$, $\dot{e}_p = \dot{h}_d = 0$.

The velocity approaches zero (quasistatic limit) in the vicinity of a stall force or when $U_0 \to 0$. At quasistatic limit, regardless of any parameter choice, we find $\dot{e}_p = \dot{h}_d(t) = 0$. One should note that the vanishing of velocity may not indicate the system is at thermodynamic equilibrium as pointed out by Ge *et al*. [25]. This can be appreciated by plotting $\dot{e}_p(t)$ or $\dot{h}_d(t)$ [using Eqs. (21) and (22)] as a function of load in long time limit. For linearly decreasing temperature case, we plot $\dot{e}_p(t)$ and $\dot{h}_d(t)$ as a function of load in Fig. 5. The figure depicts that in the long time limit, both $\dot{e}_p(t)$ and $\dot{h}_d(t)$ attain a zero value at stall force.

The dependence for $\Delta S(t)$, $\Delta e_p(t)$, and $\Delta h_d(t)$ as a function of t can be explored employing Eqs. (28), (27), and (26), respectively. The expressions for $\Delta h_d(t)$, $\Delta S(t)$, and $\Delta e_p(t)$ are lengthy and will not be presented in this work. As shown in Figs. 6(a) and 6(b), for a system that operates between hot and cold reservoirs, $\Delta h_d(t)$ and $\Delta e_p(t)$ approach a nonequilibrium steady state in the long time limit. However, for a system that operates in heat baths where its temperature decreases linearly, $\Delta S(t)$ and $\Delta e_p(t)$ increase linearly as time progresses. This reveals that, unlike systems that operate between hot and cold reservoirs, this system exhibits a higher level of irreversibility. Next we explore the dependence of the free energy dissipation rate shown in Eqs. (43) and (44) on t.
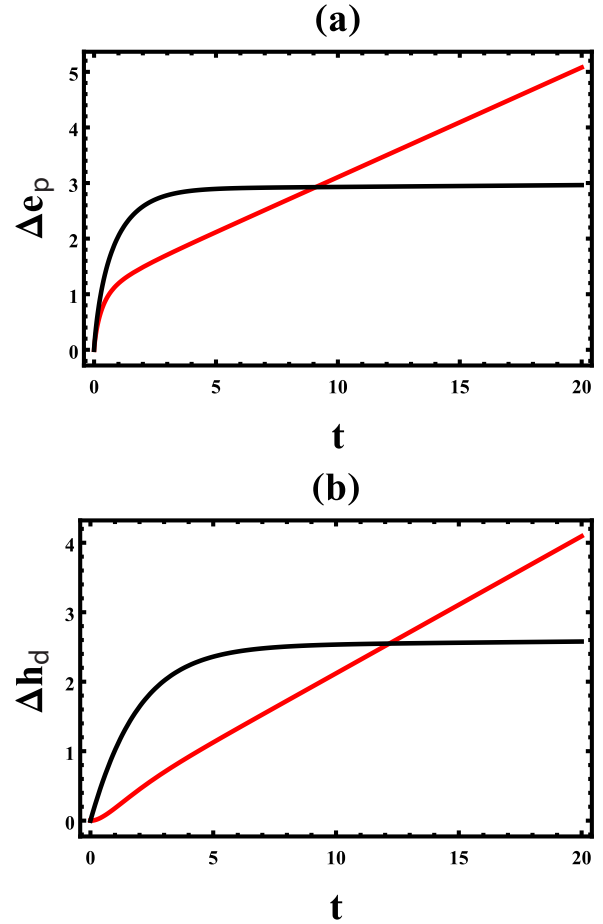

FIG. 6. (a) $\Delta e_p(t)$ as a function of t that evaluated analytically via Eq. (27) for fixed $\epsilon = 2.0$, $\tau = 20.0$ and $\lambda = 0.6$. (b) $\Delta h_d(t)$ as a function of t is plotted using Eq. (26) for fixed $\epsilon = 2.0$, $\tau = 20.0$ and $\lambda = 0.6$. In the figures, the red line shows the plot for a linearly decreasing temperature case and the black line is plotted by considering a Brownian particle that operates between the hot and cold baths.

In general $\dot{F} < 0$ and approaches zero in the long time limit for both cases (see Fig. 7).

As discussed before, once the expressions for $\dot{H}_d(t)$, $\dot{E}_p$, $\dot{S}^T$ are analyzed, the corresponding entropy balance equation can be calculated as $\frac{dS^T(t)}{dt} = \dot{E}_p - \dot{H}_d$. The expressions for these relations are very complicated. In Fig. 8, using Eqs. (36) and (37), we plot $\Delta H_d(t)$ and $\Delta E_p(t)$ as a function of t for fixed $\epsilon = 2.0$, $\tau = 20.0$ and $\lambda = 0.6$. In the figure, the red line shows the plot for a linearly decreasing temperature case, and the black line is plotted by considering a Brownian particle that operates between the hot and cold baths. Surprisingly, although $\Delta E_p(t)$ and $\Delta H_d(t)$ saturate to a constant value for a heat engine that operates between the hot and cold heat baths, for linearly decreasing temperature case both $\Delta E_p(t)$ and $\Delta H_d(t)$ step up in time linearly. This justifies that, unlike systems that operate between hot and cold reservoirs, systems that operate in heat baths where their temperature decreases linearly have a higher level of irreversibility.

Exploiting Eq. (45), let us now investigate further how the free energy behaves as a function of the system parameters. Figure 9(a) depicts the plot for the change in free energy ΔF
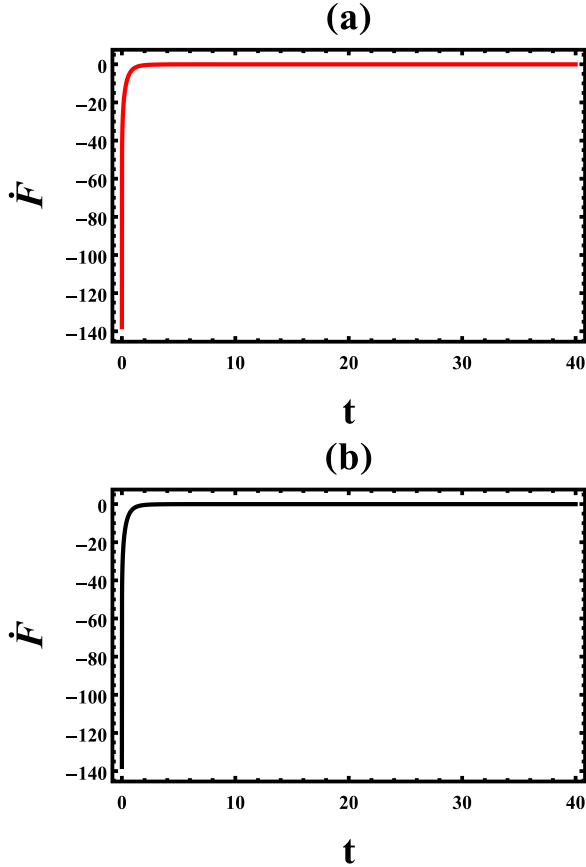
(a)

(b)

FIG. 7. (a) The free energy dissipation rate $\dot{F}$ versus t for a linearly decreasing temperature case is plotted using Eq. (43). (b) The free energy dissipation rate $\dot{F}$ as a function of t for a heat bath that coupled with the hot and cold temperature employing Eqs. (43) and (44). For both figures, the parameters are fixed as $\epsilon = 2.0$, $\tau = 20.0$ and $\lambda = 0.6$.
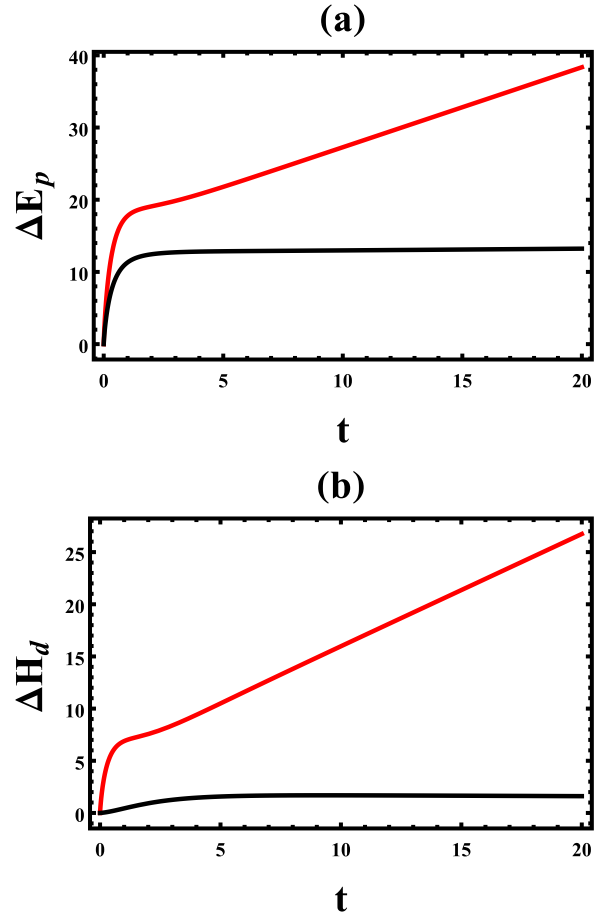
(a)

(b)

FIG. 8. (a) $\Delta E_p(t)$ as a function of t is evaluated via Eq. (37). (b) The plot of $\Delta H_d(t)$ versus t is plotted employing Eq. (36). In the figures, the parameters are fixed as $\epsilon = 2.0$, $\tau = 20.0$ and $\lambda = 0.6$. For both figures, the red line shows the plot for a linearly decreasing temperature case and the black line is plotted by considering a Brownian particle that operates between the hot and cold baths.

versus t for the system that operates between the hot and cold baths. On the other hand, Fig. 9(b) shows the plot for the change in free energy ΔF versus t for the system that operates in a linearly decreasing temperature profile. The fact that $\Delta F \neq 0$, indicates that our model system is inherently irreversible even within the long time limit. The change in free energy ΔF decreases in time and saturates to a constant but minimal value for the system that operates between the hot and cold baths. On the contrary, for the system that operates in a linearly decreasing temperature case, the change in free energy decreases linearly indicating that the degree of irreversibility is higher for such systems.

IV. THE EFFICIENCY AND VELOCITY OF THE HEAT ENGINE

As discussed before, in the presence of external force, the velocity approaches zero $V(t) = 0$ in the vicinity of the stall force. For the Brownian heat engine that operates between two heat baths, the stall force is given as

$$f = \frac{E\left(\frac{T_h}{T_c} - 1\right)}{\left(2\frac{T_h}{T_c} + 1\right)}, \tag{48}$$

while for linearly decreasing thermal arrangement case, the stall force is calculated as

$$f = \frac{E(T_h - T_c)(4T_h + T_c)}{\left(2T_h^2 + T_c^2 + 6T_cT_h\right)}. \tag{49}$$

Evaluating E_p near the stall force, one finds $E_p = 0$ as long as the system is at a steady-state regime. Far from a steady-state regime (even in the vicinity of the stall force), $E_p > 0$ which is expected as the engine operates irreversibly. For isothermal case without load, $E_p = 0$ at stationary state. Next, we explore the dependence of the velocity and efficiency on the system parameters.

A. The particle's velocity

The velocity of the particle is sensitive to time. Our analysis indicates that the velocity of the particle depends on system parameters. For instance, the velocity of the particle is positive when $T_h \neq T_c$ and $f = 0$. For isothermal case $V < 0$ as long as $f > 0$. In general for $T_h \neq T_c$ and $f > 0$, the system exhibits fascinating dynamics where $V > 0$ when the load is less than the stall force f', $f < f'$ and $V < 0$ if $f > f'$. This
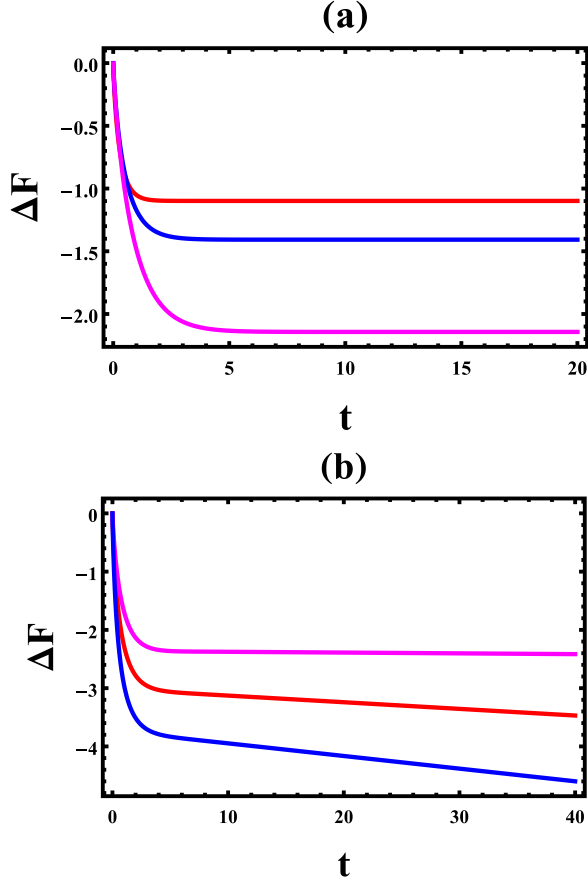
(a)

(b)

FIG. 9. (a) The change in free energy ΔF versus t is plotted using Eq. (45) for the system that operates between the hot and cold baths. The figure depicts that at a steady-state, the free energy saturates to a constant but minimal value. (b) (b) shows the dependence the change in free energy ΔF versus t for the system that operates in a linearly decreasing temperature profile. The figure depicts that as time progresses, the free energy decreases linearly. In both figures, the load is fixed as $\lambda = 0.2$. The barrier height is also fixed as $\epsilon = 0$, $\epsilon = 1.0$ and $\epsilon = 2.0$ from the top to bottom.
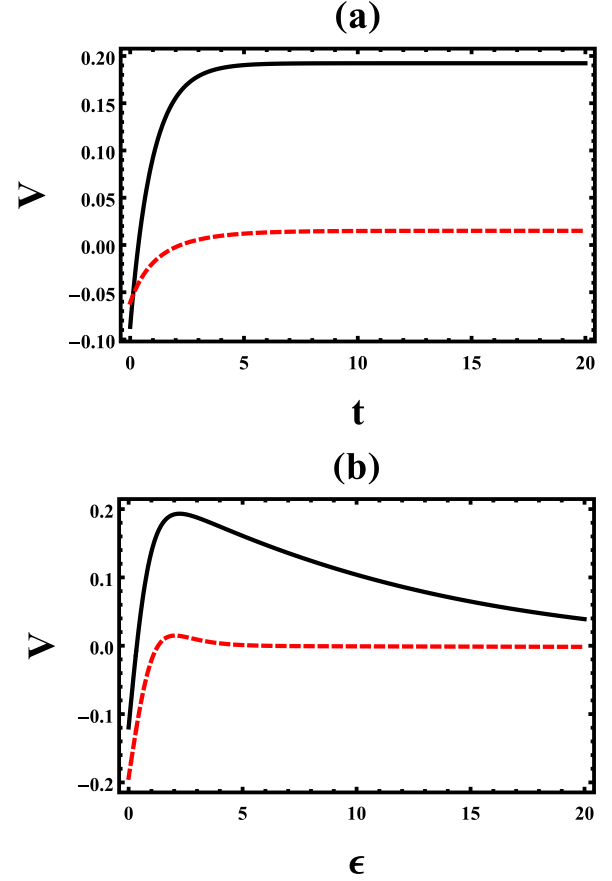
(a)

(b)

FIG. 10. (a) Particle velocity V as a function of t is plotted via Eqs. (7) or (19) for fixed $\epsilon = 2.0$, $\tau = 20.0$ and $\lambda = 0.6$ (b) Particle velocity V as a function of ϵ is analized employing via Eqs. (7) or (19) for fixed $t = 10.0$, $\tau = 20.0$ and $\lambda = 0.6$. In both figures, the black solid line indicates the plot for a heat bath where its temperature linearly decreases while the red dashed line is plotted by considering a Brownian particle that operates between the hot and cold baths.

suggests that the mobility of the particle can be manipulated by varying the external force.

The dependence of the velocity on time is also explored via Eqs. (7) or (19). The time t dictates the magnitude and the direction of the velocity. This can be appreciated by plotting V as a function of time [see Fig. 10(a)]. Figure 10(a) depicts that for small t, the net particle flow is in the reverse direction (negative). As time increases, the magnitude of V increases and saturates to a constant value. The particle velocity is significantly higher for the Brownian particle that operates in the thermal bath where its temperature decreases linearly than a Brownian particle that operates between two heat baths. In the figure, we set $\epsilon = 2.0$, $\tau = 20.0$, and $\lambda = 0.6$. In both figures, the black solid line indicates the plot for a heat bath where its temperature linearly decreases while the red line is plotted by considering a Brownian particle that operates between the hot and cold baths.

Exploiting Eqs. (7) or (19) further, in Fig. 10(b) we plot the velocity V as a function of ϵ. The figure depicts that the particle manifests a peak velocity at a particular barrier

height ϵ^{max} and at this particular height, the engine operates with maximum power. Once again the particle velocity is considerably higher for the Brownian particle that operates in the thermal bath where its temperature decreases linearly than a Brownian particle that operates between two heat baths. In the figure, we set $t = 10.0$, $\tau = 20.0$, and $\lambda = 0.6$.

The dependence for the velocity V on load is explored employing Eq. (19) as shown in Fig. 11. In the figure, we fix $t = 10.0$, $\epsilon = 2.0$, and $\lambda = 0.6$. The figure depicts that as long as the load is less than the stall force, $V > 0$ while when the load is greater than the stall force, $V < 0$. At stall force, the particle velocity becomes zero. On the other hand, the velocity steps up as the τ increases as depicted in Fig. 11(b).

B. The efficiency of the heat engine

Let us now explore how the efficiency η behaves as the model parameters vary. For both cases, the rate of work done is given as $\dot{W} = fV(t)$. On the contrary, the rate of heat input is model dependent. For the case where the system operates between the two baths, the rate of heat input is given as
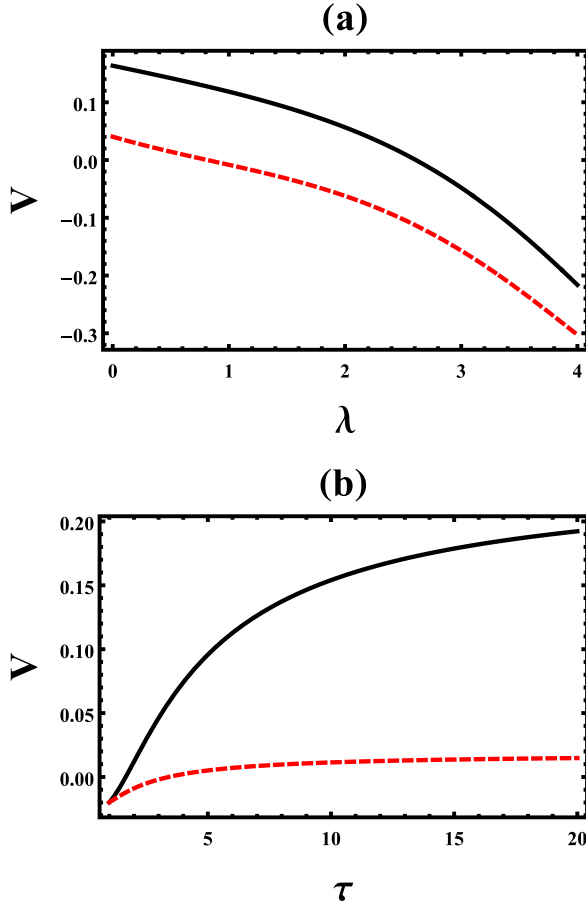
(a)

(b)

FIG. 11. (a) The particle velocity V as a function of λ is evaluated via Eqs. (7) or (19) for fixed $\epsilon = 2.0$, $\tau = 8.0$ and $t = 10.0$. (b) The particle velocity V as a function of τ is plotted employing Eqs. (7) or (19) for fixed $t = 10.0$, $\epsilon = 2.0$ and $\lambda = 0.6$. In figures, the black solid line indicates the plot for a heat bath where its temperature linearly decreases while the red dashed line is plotted by considering a Brownian particle that operates between the hot and cold baths.

(a)

(b)

FIG. 12. (a) The efficiency η as a function of λ evaluated using Eq. (50) for fixed values of $\epsilon = 2$, $\tau = 2.0$ and $t = 1000.0$. (b) The efficiency η as a function of ϵ is plotted employing Eq. (50) for fixed values of $t = 1000.0$, $\tau = 2.0$ and $\lambda = 0.2$. The bottom line represents the plot for linearly decreasing temperature case while the top line is plotted for a heat engine that operates between the hot and cold baths.

$\dot{Q}_{in}(t) = \dot{Q}_h(t) = T_h(p_2 P_{32} - p_3 P_{23}) \ln(\frac{P_{32}}{P_{23}})$. For linearly decreasing temperature case, since the heat bath from the left potential well contributes for the particle to jump to the right, the particle must get $\dot{Q}_{in}(t) = T_h(p_2 P_{32} - p_3 P_{23}) \ln(\frac{P_{32}}{P_{23}}) + T_c(p_2 P_{12} - p_1 P_{21}) \ln(\frac{P_{12}}{P_{21}})$ amount of heat from the system. The efficiency then is given by

$$\eta = \frac{\dot{W}}{\dot{Q}_{in}(t)}. \tag{50}$$

In general, the efficiency of the system increases in time and at a steady state, the system attains maximum efficiency. The efficiency at the quasistatic limit can be obtained via Eq. (50). For a Brownian heat engine that operates between two heat baths, one gets

$$\eta = 1 - \frac{T_c}{T_h}, \tag{51}$$

which is the efficiency of the Carnot heat engine. For the heat engine that operates in a heat bath that decreases linearly, at
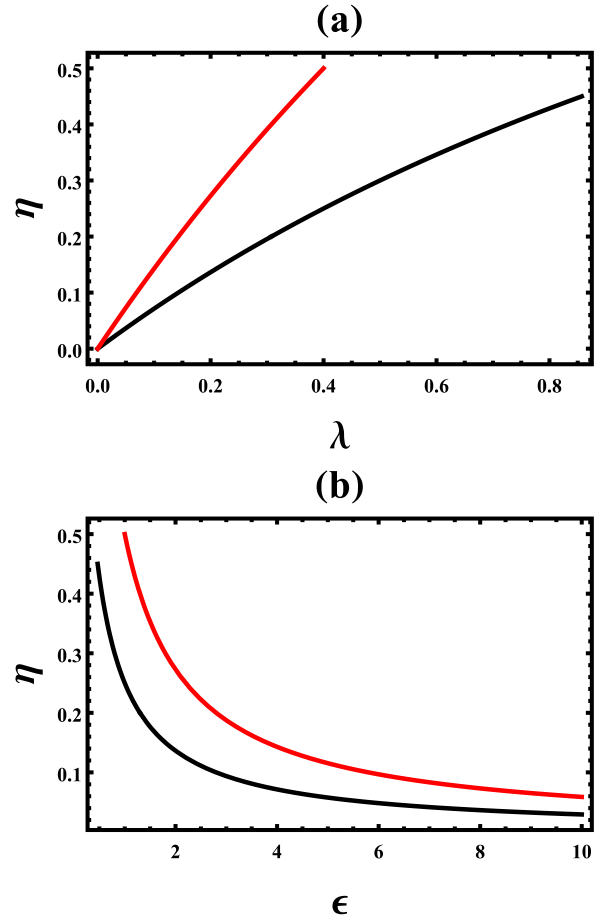
the quasistatic limit, we get

$$\eta = 1 - \frac{(T_c(T_c + 5T_h))}{(2T_h(T_c + 2T_h))}, \tag{52}$$

which is approximately equal to the efficiency of the endorevresible heat engine η_{CA}

$$\eta_{CA} = 1 - \sqrt{T - c/T_h}, \tag{53}$$

as long as the temperature difference between the hot and the cold reservoirs is not large. This can be further appreciated by Taylor expanding Eqs. (52) and (53) around $\tau = 1$. As discussed in Ref. [20], it is still unknown why different model systems approach the Taylor expression shown above.

The dependence of the efficiency η on the model parameters is also explored by omitting the heat exchange via kinetic energy. The efficiency η as a function of rescaled load is evaluated analytically [see Fig. 12(a)] via Eq. (50). The figure is plotted by fixing $\epsilon = 2.0$, $\tau = 2.0$, and $t = 1000.0$. The figure exhibits that η increases to its maximum (quasistatic limit) value. The efficiency is considerably large for

the system that operates between two heat baths. The efficiency η as a function of barrier height is plotted in Fig. 12(b) for the parameter values of $\lambda = 0.2$, $\tau = 2.0$, and $t = 1000.0$. The efficiency decreases as the barrier height increases. When the magnitude of the rescaled temperature steps up, the efficiency of the system monotonously increases.

V. SUMMARY AND CONCLUSION

Studying the thermodynamic feature of nonequilibrium systems is challenging since their energy as well as the particles' flux constantly changes in time. Consequently, exploring the thermodynamics feature of non-equilibrium systems requires a more general concept as well as rigorous mathematical analysis. Due to the lack of exact solutions, most of the previous works addressed how different thermodynamics features behave either at the quasistatic limit or at steady-state regimes. To fill this gap, in this work, we present an exactly solvable model that helps to explore the thermodynamic features of systems beyond a linear response and steady-state regime. Not only the long-time property (steady-state) but also the short-time behavior of the system is explored by obtaining exact time-dependent solutions. The general expressions for free energy, entropy production as well as entropy extraction rates are derived for a system that is genuinely driven out of equilibrium by time-independent force as well as by spatially varying thermal background.

From an equilibrium thermodynamics point of view, the entropy $S(t)$ is the most explored physical quantity. It is a well-known fact that even in the absence of symmetry-breaking fields, the entropy of systems can be greater than zero $S(t) > 0$ as long as the system operates in a finite time and only in a long time limit does the system become reversible $S(t) = 0$. However, in the presence of symmetry-breaking fields, the systems are driven out of equilibrium even within the long time limit. In this regard, most of the previous studies focused on exploring how the entropy $S(t)$, the production $\dot{e}_p(t)$ and extraction rates $\dot{h}_d(t)$ behave either at steady state or the quasistatic limit. To comprehend the thermodynamic features of systems beyond a linear response and the steady-state regime, we solve the model system analytically. The thermodynamic properties of a system that operates between the hot and cold baths are also compared and contrasted (as a function of time) with a system that operates in a heat bath where its temperature linearly decreases along with the reaction coordinate. For our model system, the fact that the entropy, the entropy production, and extraction rate are greater than zero suggests that in the presence of symmetry-breaking fields such as nonuniform temperature or external force, the system is driven out of equilibrium. The entropy production $\dot{e}_p(t)$ and extraction rates $\dot{h}_d(t)$ are also considerably larger for the linearly decreasing temperature case than the entropy for Brownian particle that operates between the hot and cold baths. This suggests that the degree of irreversibility is higher for the system that operates in a heat bath where its temperature decreases linearly along with the reaction coordinate.

According to the celebrated statistical thermodynamics theory, systems tend to maximize their entropy or minimize their free energy in the effort to reach thermal equilibrium, and consequently, the change in free energy $\Delta F = 0$. This also implies for any irreversible system, the free energy difference is a positive thermodynamic quantity. To discern the thermodynamic features of systems beyond the equilibrium regime, we further explore the dependence of free energy on the system parameters for a system that is genuinely driven out of equilibrium. For our system, $\Delta F \neq 0$ and this indicates that our model system is inherently irreversible even within the long time limit. The change in free energy ΔF decreases in time and saturates to a constant but minimal value for the system that operates between the hot and cold baths. On the contrary, for the system that operates in a linearly decreasing temperature case, the change in free energy decreases linearly indicating that the degree of irreversibility is higher for such a system. The term that is related to entropy production rate ($\Delta E_p(t)$) and the heat dissipation rate ($\Delta H_d(t)$) saturates to a constant value for a heat engine that operates between the hot and cold heat baths. Surprisingly for the linearly decreasing temperature case both $\Delta E_p(t)$ and $\Delta H_d(t)$ step up in time linearly. This justifies that, unlike systems that operate between hot and cold reservoirs, systems that operate in a heat bath where its temperature decreases linearly have a higher level of irreversibility.

The energetics of the system that operates between the hot and cold baths are also compared and contrasted with a system that operates in a heat bath where its temperature linearly decreases along the reaction coordinate. We show that a system that operates between the hot and cold baths has significantly lower velocity but a higher efficiency in comparison with a linearly decreasing case. For a linearly decreasing background temperature case, we show that the efficiency of such a Brownian heat engine is lower than Carnot's efficiency even at the quasistatic limit. At the quasistatic limit, the efficiency of the heat engine approaches the efficiency of the endoreversible engine.

Due to the lack of exact analytic results, most of the previous work studied the thermodynamic features of systems in a linear response and steady-state regime. The exactly solvable model presented in this work enables us to explore how the free energy, total entropy, entropy production, and extraction rates behave as a function of time far beyond linear response and steady-state regime. The change in free energy in particular exhibits an elegant time dependence. Only for a linearly decreasing thermal arrangement does the free energy monotonously decrease in time revealing the way the temperature is arranged in the reaction coordinate affects the free energy. In conclusion, even though a specific model system is considered, the thermodynamic relations that are obtained in this work are generic and vital to advance the nonequilibrium statistical mechanics.

APPENDIX A: BROWNIAN PARTICLE THAT OPERATES BETWEEN TWO BATHS

In this Appendix we will give the expressions for $p_1(t)$, $p_2(t)$, and $p_3(t)$ as well as $V(t)$ for a Brownian particle that

operates between the hot and cold baths. For the particle which is initially situated at site $i = 1$, the time dependent normalized probability distributions after solving the rate equation $\frac{d\vec{p}}{dt} = \mathbf{P}\vec{p}$ are calculated as

$$p_1(t) = c_1 \frac{a(2 + vb)}{\mu(\mu + (a^2 + \mu)vb)}$$
$$+ c_2 e^{-\frac{(a+a^2\mu+\mu^2)t}{2a}}\left(-1 + \frac{a(-1 + a\mu)}{-\mu^2 + avb}\right), \quad \text{(A1)}$$

$$p_2(t) = -c_3 e^{\frac{1}{2}t(-2-vb)} - c_2 \frac{a\, e^{-\frac{(a+a^2\mu+\mu^2)t}{2a}}(-1 + a\mu)}{-\mu^2 + avb}$$
$$+ c_1 \frac{(2a^2 + \mu)}{\mu + (a^2 + \mu)vb}, \quad \text{(A2)}$$

$$p_3(t) = c_1 + c_2 e^{-\frac{(a+a^2\mu+\mu^2)t}{2a}} + c_3 e^{\frac{1}{2}t(-2-vb)}, \quad \text{(A3)}$$

where

$$c_1 = \frac{\mu(\mu + (a^2 + \mu)vb)}{(a + a^2\mu + \mu^2)(2 + vb)}, \quad \text{(A4)}$$

$$c_2 = -\frac{a}{(a + a^2\mu + \mu^2)\left(-1 + \frac{a(-1+a\mu)}{-\mu^2+avb}\right)}, \quad \text{(A5)}$$

$$c_3 = -\frac{\mu(\mu + a^2vb + \mu vb)}{(a + a^2\mu + \mu^2)(2 + vb)}$$
$$+ \frac{a}{(a + a^2\mu + \mu^2)\left(-1 + \frac{a(-1+a\mu)}{-\mu^2+avb}\right)}. \quad \text{(A6)}$$

Here $\sum_{i=1}^{3} p_i(t) = 1$ revealing the probability distribution is normalized. In the limit of $t \to \infty$, we recapture the steady state probability distributions

$$p_1^s = \frac{a}{a + a^2\mu + \mu^2}, \quad \text{(A7)}$$

$$p_2^s = \frac{\mu(2a^2 + \mu)}{(a + a^2\mu + \mu^2)(2 + bv)}, \quad \text{(A8)}$$

$$p_3^s = \frac{\mu(\mu + b(a^2 + \mu)v)}{(a + a^2\mu + \mu^2)(2 + bv)}. \quad \text{(A9)}$$

The velocity $V(t)$ at any time t is the difference between the forward $V_i^+(t)$ and backward $V_i^-(t)$ velocities at each site i

$$V(t) = \sum_{i=1}^{3}(V_i^+(t) - V_i^-(t))$$
$$= (p_1 P_{21} - p_2 P_{12}) + (p_2 P_{32} - p_3 P_{23})$$
$$+ (p_3 P_{13} - p_1 P_{31}). \quad \text{(A10)}$$

Exploiting Eq. (63), one can see that the particle attains a unidirectional current when $f = 0$ and $T_h > T_c$. For isothermal case $T_h = T_c$, the system sustains a nonzero velocity in the presence of load $f \neq 0$ as expected. Moreover, when $t \to \infty$, the velocity $V(t)$ increases with t and approaches the steady state velocity

$$V^s = 3\frac{\mu\left(bav - \frac{\mu}{a}\right)}{2(2 + vb)\left(1 + a\mu + \frac{\mu^2}{a}\right)}. \quad \text{(A11)}$$

APPENDIX B: BROWNIAN PARTICLE THAT OPERATES IN A LINEARLY DECREASING TEMPERATURE

The expressions for $p_1(t)$, $p_2(t)$, and $p_3(t)$ as well as $V(t)$ are derived considering a Brownian particle that operates in a heat bath where its temperature decreases linearly along with the reaction coordinate. For the particle which is initially situated at site $i = 1$, the time-dependent normalized probability distributions after solving the rate equation $\frac{d\vec{p}}{dt} = \mathbf{P}\vec{p}$ are given as

$$p_1 = \frac{a_2(2 + v)}{\mu_2^2 + a_1 a_2 \mu_1 v + \mu_2^2 v} c_1$$
$$+ \left(-1 + \frac{-a_2 + a_1 a_2 \mu_1}{-\mu_2^2 + a_2 v}\right)e^{[t(\frac{-a_2-a_1 a_2\mu_1-\mu_2^2}{2a_2})]} c_2$$
$$\text{(B1)}$$

$$p_2 = -\frac{-2a_1 a_2 \mu_1 - \mu_2^2}{\mu_2^2 + a_1 a_2 \mu_1 v + \mu_2^2 v} c_1$$
$$- \frac{-a_2 + a_1 a_2 \mu_1}{-\mu_2^2 + a_2 v} e^{[t(\frac{-a_2-a_1 a_2\mu_1-\mu_2^2}{2a_2})]} c_2 - e^{[t\frac{1}{2}(-2-v)]} c_3$$
$$\text{(B2)}$$

$$p_3 = c_1 + e^{[t(\frac{-a_2-a_1 a_2\mu_1-\mu_2^2}{2a_2})]} c_2 + e^{[\frac{1}{2}(-2-v)t]} c_3, \quad \text{(B3)}$$

where

$$c_1 = -\frac{-\mu_2^2 - a_1 a_2 \mu_1 v - \mu_2^2 v}{(a_2 + a_1 a_2 \mu_1 + \mu_2^2)(2 + v)}, \quad \text{(B4)}$$

$$c_2 = -\frac{a_2(-\mu_2^2 + a_2 v)}{(a_2 + a_1 a_2 \mu_1 + \mu_2^2)(-a_2 + a_1 a_2 \mu_1 + \mu_2^2 - a_2 v)}, \quad \text{(B5)}$$

$$c_3 = \frac{\mu_2^2 - 2a_2 v + a_1 a_2 \mu_1 v + \mu_2^2 v - a_2 v^2}{(2 + v)(a_{12} - a_1 a_2 \mu_1 - \mu_2^2 + a_2 v)}. \quad \text{(B6)}$$

Once again, $\sum_{i=1}^{3} p_i(t) = 1$ revealing the probability distribution is normalized. When $t \to \infty$, the steady state probability distributions converge to

$$p_1^s = \frac{a_2}{(a_2 + a_1 a_2 \mu_1 + \mu_2^2)}, \quad \text{(B7)}$$

$$p_2^s = \frac{(2a_1 a_2 \mu_1 + \mu_2^2)}{((a_2 + a_1 a_2 \mu_1 + \mu_2^2)(2 + v))}, \quad \text{(B8)}$$

$$p_3^s = \frac{(a_1 a_2 \mu_1 v + \mu_2^2(1 + v))}{((a_2 + a_1 a_2 \mu_1 + \mu_2^2)(2 + v))}. \quad \text{(B9)}$$

The velocity $V(t)$ at any time t is the difference between the forward $V_i^+(t)$ and backward $V_i^-(t)$ velocities at each site i

$$V(t) = \sum_{i=1}^{3}(V_i^+(t) - V_i^-(t))$$
$$= (p_1 P_{21} - p_2 P_{12}) + (p_2 P_{32} - p_3 P_{23})$$
$$+ (p_3 P_{13} - p_1 P_{31}). \quad \text{(B10)}$$

In the limit $t \to \infty$, the velocity $V(t)$ increases with t and approaches to steady state velocity

$$V^s = \frac{(3(-\mu_2^2 + a_1 a_2 \mu_1 v))}{(2(a_2 + a_1 a_2 \mu_1 + \mu_2^2)(2 + v))}. \quad \text{(B11)}$$

[1] H. Ge and H. Qian, Phys. Rev. E **81**, 051133 (2010).

[2] T. Tome and M. J. de Oliveira, Phys. Rev. Lett. **108**, 020601 (2012).

[3] J. Schnakenberg, Rev. Mod. Phys. **48**, 571 (1976).

[4] T. Tome and M. J. de Oliveira, Phys. Rev. E **82**, 021120 (2010).

[5] R. K. P. Zia and B. Schmittmann, J. Stat. Mech. (2007) P07012.

[6] U. Seifert, Phys. Rev. Lett. **95**, 040602 (2005).

[7] T. Tome, Braz. J. Phys. **36**, 1285 (2006).

[8] G. Szabo, T. Tome, and I. Borsos, Phys. Rev. E **82**, 011105 (2010).

[9] B. Gaveau, M. Moreau, and L. S. Schulman, Phys. Rev. E **79**, 010102(R) (2009).

[10] J. L. Lebowitz and H. Spohn, J. Stat. Phys. **95**, 333 (1999).

[11] D. Andrieux and P. Gaspar, J. Stat. Phys. **127**, 107 (2007).

[12] R. J. Harris and G. M. Schutz, J. Stat. Mech. (2007) P07020.

[13] T. Tome and M. J. de Oliveira, Phys. Rev. E **91**, 042140 (2015).

[14] Luo Jiu-li, C. Van den Broeck, and G. Nicolis, Z. Phys. B **56**, 165 (1984).

[15] Chung Yuan Mou, J.-L. Luo, and G. Nicolis, J. Chem. Phys. **84**, 7011 (1986).

[16] C. Maes and K. Netocny, J. Stat. Phys. **110**, 269 (2003).

[17] L. Crochik and T. Tome, Phys. Rev. E **72**, 057103 (2005).

[18] M. Asfaw, Phys. Rev. E **89**, 012143 (2014).

[19] M. Asfaw, Phys. Rev. E **92**, 032126 (2015).

[20] K. Brandner, M. Bauer, M. Schmid, and U. Seifert, New J. Phys. **17**, 065006 (2015).

[21] B. Gaveau, M. Moreau, and L. S. Schulman, Phys. Rev. E **82**, 051109 (2010).

[22] E. Boukobza and D. J. Tannor, Phys. Rev. Lett. **98**, 240601 (2007).

[23] Mesfin Asfaw Taye, Phys. Rev. E **94**, 032111 (2016).

[24] Mesfin Asfaw Taye, Phys. Rev. E **101**, 012131 (2020).

[25] H. Ge, Phys. Rev. E **89**, 022127 (2014).

[26] Hyun Keun Lee, C. Kwon, and H. Park, Phys. Rev. Lett. **110**, 050602 (2013).

[27] T. Bameta, D. Das, D. Das, R. Padinhateeri, and M. M. Inamdar, Phys. Rev. E **95**, 022406 (2017).

[28] D. Oriola and J. Casademunt, Phys. Rev. Lett. **111**, 048103 (2013).

[29] O. Campàs, Y. Kafri, K. B. Zeldovich, J. Casademunt, and J.-F. Joanny, Phys. Rev. Lett. **97**, 038101 (2006).

[30] Mesfin Asfaw Taye, J. Stat. Phys. **169**, 423 (2017).